Materials Advances

ROYAL SOCIETY OF CHEMISTRY

REVIEW

View Article Online
View Journal | View Issue

Cite this: *Mater. Adv.*, 2022, 3, 4460

Metal-free triboelectric nanogenerators for application in wearable electronics

Giovanni da Silva Oliveira, Iuri Custodio Montes Candido and Helinando Pequeno de Oliveira *

Received 19th February 2022,
Accepted 24th April 2022

DOI: 10.1039/d2ma00195k

rsc.li/materials-advances

The development of self-powered systems applied in wearable electronics based on triboelectric nanogenerators introduces advances in the internet of Things, wireless communication, and biomedical fields. For this, efforts have been conducted to substitute metal-based electronics with non-conventional components such as conducting polymers, carbon derivatives, and inonogels providing better wearability, comfort, self-healability, mechanical resistance, and ease of integration with textiles. In particular, the conversion of pulsed output in triboelectric nanogenerators into DC power is helpful to drive electronics by the direct association of energy harvesting systems and energy storage devices that can be assembled in the same framework (metal-free electrodes). In this review, the multifunctionality of metal-free TENGs is discussed in light of the development of new autonomous wearable devices.

Introduction

The development of the Internet of Things and the progressive interconnections of data from embedded devices (for the following exchange of data to the internet[1–3]) depends on the adequate integration of portable and flexible electronics with the body, as a part of requisites for the production of self-powered devices with implication on artificial electronic skins and motion tracking sensors[4–8] in which data from the body (movement, foot activity, breathing[4,7,9,10]) and environmental conditions such as temperature, pressure and humidity[11] are monitored, recorded and transferred to the internet.

As a consequence, the integration of flexible electronics with clothes and the body is a critical step for the production of smart and multifunctional devices.[9] The common drawback for these applications is the limitation of energy storage devices to power up these wearable electronics. Conventional lithium-ion batteries are expensive and characterized as bulky volume devices (rigid framework, heavy package, and non-environmentally friendly behavior)[4,12,13] introducing potential hazards for human health[14] and several consequences on comfort and environmental issues.

The required minimal dependence on devices with energy storage devices reinforces the necessity of the strategies to

Institute of Materials Science, Federal University of São Francisco Valley, Avenida Antônio Carlos Magalhães, 510 - Santo Antônio CEP: 48902-908, Juazeiro/BA, Brazil. E-mail: helinando.oliveira@univasf.edu.br

Giovanni da Silva Oliveira

Giovanni da Silva Oliveira is a graduate student (MSc degree) in materials science at the Universidade Federal do Vale do São Francisco and is undergoing research about triboelectric nanogenerators.

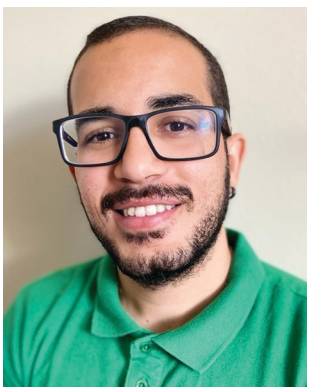

Iuri Custodio Montes Candido

Iuri C. M. Candido is a graduate student (DSc degree) in materials science at the Universidade Federal do Vale do São Francisco and is undergoing research about triboelectric nanogenerators.

harvest energy from the environment or the body movement. If it is considered that a few hundred watts can be collected from the mechanical movement of the body throughout the day, the production of wearable harvesting systems is critical for the development of integrated devices. Also, it is worth mentioning that harvested electrical signals can be applied as an input for transduction sensors, inhibiting additional external sources to drive portable electronics.[11]

Among the energy harvesting prototypes, triboelectric nanogenerators (TENGs) are one of the most promising electronics devices. Invented by Wang and coworkers in 2012,[15] TENGs rapidly attracted much attention in the literature[15–20] due to the viability of conversion of the mechanical energy into an electrical signal, making the direct conversion of mechanical movement into electric signals[21–23] for biomedical applications[24–26] and bioelectronic systems possible.[27] Due to this safe generation, the use of TENGs as generators of high voltage (in order of kV) with a small current has been preferable, as an example, for the development of a refreshable display for portable e-books for the blind – the TENG is connected to a refreshable Braille display.[28]

As a principle of operation, a typical TENG-based device is activated by the contact/separation of two different surfaces with the ability to accumulate oppositely charged species. The assembly of the device depends on the disposition of tribonegative and tribopositive pairs and supporting collectors (electrodes) that conduct the generated current to an external load.[29–34] The big challenge to incorporating TENGs into wearables is the integration of conductive components and active tribopairs into cotton, wool, silk, or elastomers without sacrificing the intrinsic characteristics of the original textile in terms of breathable and fashionable properties.[10,13,35–37]

One of the most common strategies to develop electrodes for wearable TENGs is based on the modification of garments with metal layers, such as the modification of polyester with Ni film,[38] from the incorporation of copper,[39–41] aluminum,[42–44] ITO[45] and gold.[46–48] However, the modification of textiles with metal derivatives introduces high cost in the overall production process,[19,49] which is combined with disadvantages of characteristic high weight, low wearability and non-environmentally friendly behavior.[19,50–52]

In addition, the mechanical fragility of the metallic electrode layer for TENGs is critical for applications involving contact with the body (such as in muscle motion detection) since the metal layer introduces constraints in tissue-based applications. To circumvent these drawbacks, the use of an ionic hydrogel introduces adhesion ability, stretchability and superior self-healing properties.[53]

Alternatives to the metal coating layers have been considered from the use of conductive organic polymers (CPs), such as polypyrrole (PPy),[52,54,55] polyaniline (PANI),[10,17,56,57] poly(3,4-ethylene dioxythiophene:polystyrene sulfonate) (PEDOT:PSS)[9,14,58–60] prepared by different methods: *in situ*, interfacial, and vapor deposition[52,56,61–64] and carbon derivatives such as carbon nanotubes and graphene oxide, *etc.*[65–67] deposited on textiles, elastomers or electrospun fibers.

These materials can be explored in a harvesting-storage-in-one system in which TENGs are integrated with energy storage devices. In particular, the conversion of pulsed electrical output into DC power is required to drive electronics.[68] The sharing in the electrodes for TENGs and energy storage devices[64,69–72] is extremely necessary for the reduction of costs and ease of integration in wearables, facilitating the use of conducting polymers (prototypes of pseudocapacitive materials) and carbon derivatives (prototypes of electrical double layer capacitive components) as good candidates for metal-free integrated TENGs-supercapacitors.

Herein, the advantages and challenges associated with the substitution of metal electrodes by polymeric/carbon coating in prototypes of triboelectric nanogenerators are discussed in terms of modes of operation, nature of electrodes and tribopairs, and strategies to connect energy harvesting systems with energy storage devices to power up different electronics.

Triboelectric nanogenerators

The development of metal-free electronic devices has been primarily considered a requisite for sustainability issues since the substitution of metallic parts of devices (such as collectors) for carbon-based materials is typically associated with improvement in the corrosion resistance, stability against oxidation and mechanical resistance.[73–75]

In particular, conventional TENGs make use of aluminum film as a metal electrode. The substitution of these structures by metal-free species avoids several drawbacks of metal-based species, such as fatigue resistance (over repeated mechanical contact), degradation *via* oxidation in humid environments, and potential corrosion in saline conditions. These conditions are common from the contact with the skin for the energy harvesting from the body movement. In addition, wearable metal-free TENGs introduce advantages relative to the limited elastic range of metallic films and poor adhesion on skin.[75]

As observed, the required high conductivity for electrodes is conveniently addressed for metal-based materials. However, the

Helinando Pequeno de Oliveira

Helinando P. de Oliveira has a Doctor of Sciences degree in Physics from the Universidade Federal de Pernambuco (Brazil, 2004). He is a full professor at the Universidade Federal do Valedo São Francisco (Brazil) and coordinates the group of Impedance Spectroscopy and Organic Materials.

mechanical properties and degradation under contact with the body (salinity and water) reinforce the required efforts to develop metal-free support with high conductivity for integration with wearables. These characteristics must match with the operation mode of the TENG device, in a configuration where metallic parts (highly conductive surfaces) are minimally necessary. In light of this, the next section is focused on the operation modes of these devices.

Working mechanisms

The working mechanisms in triboelectric nanogenerators are defined by two processes: contact electrification (CE) and electrostatic induction (EI).[76,77] The conventional mechanism is exemplified in ref. 78, in which two polymeric films are used (defined as tribomaterials), (such as polyvinylidene fluoride (PVDF) and polyvinyl alcohol (PVA)), coated by a thin layer of aluminum (Al), applied as an energy collector, in a sandwich shaped structure. After contact of two polymers through the application of a compression force, electrical charges are induced on the surfaces, and after separation, a potential difference is generated between interfaces of the collectors, causing a flow of electrons to an external load. The repetition of the relative movement between polymer layers generates an electric current in the opposite direction than the first flux. By repeating successively these cycles, an output of an alternating current is observed.[78,79]

The overall efficiency in the power generation for TENGs depends on the adequate coupling of tribopairs, with special attention to the ability to couple materials that donate and receive a high density of charges per cycle. The triboelectric series[76] is a list of materials classified from more tribopositives (that have a greater affinity to give electrons) to more tribonegative ones. The closer to the top of the list, the greater the tendency to donate charged species, on the other hand, the closer to the bottom, the greater the tendency to receive charged species – the most efficient TENG combines the tribopositive with tribonegative materials with adequate current collectors and adequate configuration (mode of operation) for each application.[80]

The most conventional methods for the energy harvesting from mechanical movements using TENGs are based on a vertical contact–separation mode, lateral sliding mode, single-electrode mode, and independent layer mode,[22,81,82] as illustrated in Fig. 1.

While the single-electrode mode is characterized by ease of integration with wearables, the free-standing mode presents high conversion efficiency but complex integration with wearables, indicating that in addition to the nature of electrodes and triboelectric active layers, the operation mode must consider the specific application. The most common operation modes on TENGs are detailed as follows.

Vertical contact-separation mode (VS mode)

The most common assembly for TENGs is based on the vertical contact–separation method (see Fig. 2) in which two tribopairs with distinct polarity are vertically disposed of in a face-to-face stacked configuration. Relative to the nature of these materials,

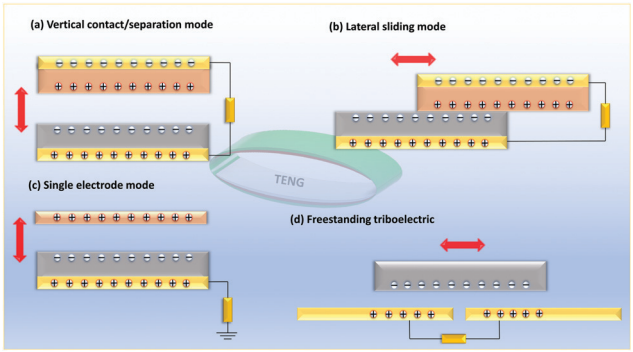

Fig. 1 Fundamental modes for TENG operation for the (a) vertical contact/separation mode, (b) lateral sliding mode, (c) single electrode mode, and (d) freestanding mode.

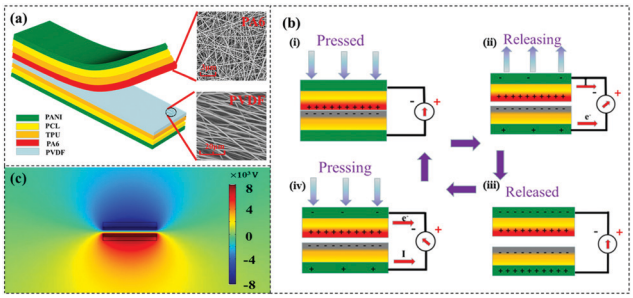

Fig. 2 (a) Disposition of the conducting layer and active triboelectric electrospun nets. (b) Scheme of the operation mode of the vertical contact–separation method in a complete cycle of contact separation and (c) simulation of the potential distribution between two triboelectric materials. Reprinted from ref. 57, Copyright (2019), with permission from Elsevier.

it is possible to combine two dielectric layers or a dielectric and a conductive triboelectric layer. In the case of tribopairs composed of two dielectric layers, the deposition of a conductive layer on the outer surface is required, to be used as a current collector. On the other hand, for an asymmetric configuration in which one electrode is electrically conductive, the outer surface deposition of the conductive film is required for just one electrode, since in this case the conductive triboactive layer can be explored as an electrode itself. Under external effort (pressing force) the two active materials get into contact and charges are generated (electrical induction) that result in two oppositely charged surfaces. Upon release, the layers tend to be separated by a small gap, creating an external potential[77,79] that forces a current to circulate in the direction of an external load. Under the application of a new cycle of compressive force on the device, the gap is closed, the potential tends toward zero and the charges flow back to establish a new equilibrium condition.[22] The resulting alternate current presents, however, an asymmetric behavior. It is a consequence of the "sticking effect", described in ref. 83 and justified by the independent ascending and descending steps of layers that are affected by the adhesion of parts due to an impulsive force that introduces asymmetric behavior in the overall output, observed

in the electrical output. The overall process described above is schematically drawn in Fig. 2. A critical point to be considered in the preservation of the cyclability of the device is the repetition conditions of contact and the full separation of pairs under successive uses that result in damage due to the continuous surface friction. Scheme from Fig. 2 (reprinted with permission from ref. 57) represents a multiple-layer assembly for wearable TENG composed of layers of PVDF (the negative triboelectric layers) and PA6 (positive triboelectric layers) with conventional cloth coated by polyaniline acting as a conductive substrate (current collector). As observed, the coating layer of polyaniline on cloth confers high conductivity to the electrodes of TENG while preserving the intrinsic properties of the clothes for the contact with the body, introducing multifunctional properties such as its intrinsic antibacterial activity.[84]

Side-slip mode (S mode)

The same configuration of tribopairs for the contact–separation mode is explored in the side-slip mode. In this assembly, the energy harvesting is established by contact–separation steps in which separation is observed from sliding between surfaces that not only creates charges but also produces a lateral polarization along the sliding direction. The created field forces the circulation of a current along with an external load and the continuous back-and-forth sliding results in an alternating electrical output for the generator. To improve the performance of this type of TENG, variations in the side-slip mode are obtained from linear movement of disk and cylindric rotation, with advantages relative to the power output in comparison with the contact–separation method,[22] while the integration with wearables represents a barrier to be considered for prototypes operating in this mode.

An interesting method that separates charges in wearable TENGs from sliding makes use of electrostatic breakdown, which is observed in wool-based fabrics in very dry weather. As schematically drawn in Fig. 3 (reprinted with permission from ref. 34), the interwoven warp yarns with wearable TENGs explore the principle of air breakdown with the contact-sliding motion mode charging the frictional electrode under contact.

Single electrode mode (SE mode)

The single electrode mode is a configuration of TENG in which the moving triboelectric layer is in contact with one electrode. The second electrode is a source of electrons (such as a grounded surface). The exchange of electrons between the moving triboelectric layer to the reference controls the potential and the assembly of the device can combine vertical and side-slip methods to favor the use of self-powered sensors. Fig. 4 shows the modified fibrous electrode coated with polypyrrole applied as a wearable electrode, the general scheme of operation under the contact–separation mechanism, and the resulting open-circuit voltage and short-circuit current as a function of different chemical treatments on a single electrode.[52] The easiest configuration of the single electrode mode facilitates the integration with wearables while the lower power output is an important issue to be addressed in the improvement of its overall performance. The reduction from two to one surface acting as an electrode for the SE mode introduces a strong

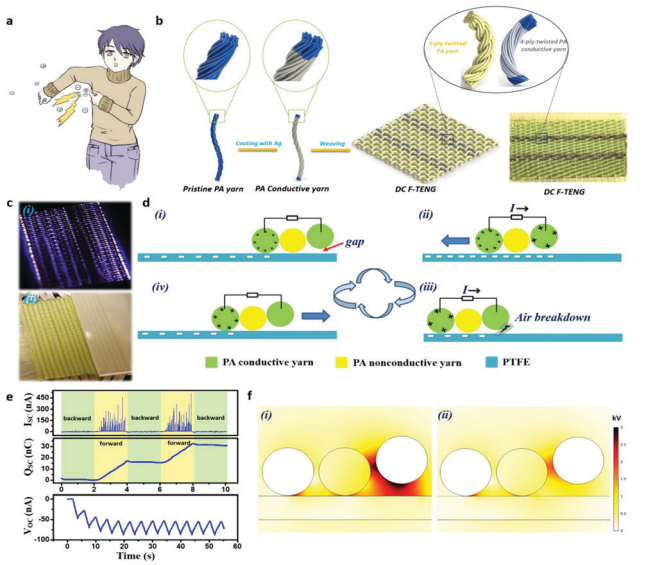

Fig. 3 Scheme of the fabrication process and working mechanism of the wearable contact-sliding TENG (a) the electrostatic breakdown in clothes, (b) the fabrication process of wearable TENG, (c) photos of the air brake under PTFE contact-sliding motion, (d) working principles of the wearable TENG, (e) electrical output performances of the device and (f) simulated electric field distribution before and after an electrostatic breakdown. Reprinted with permission from ref. 34. Copyright 2020 American Chemical Society.

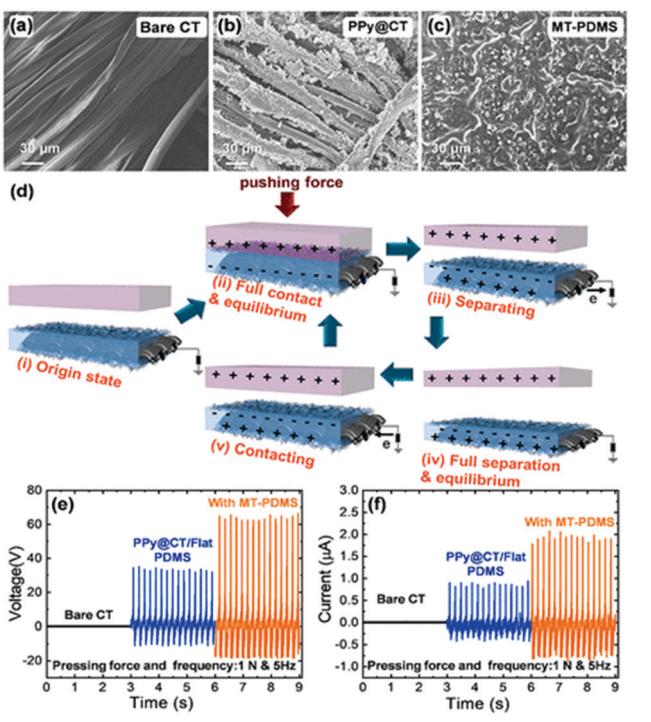

Fig. 4 SEM of textile-based electrodes (pure and chemically modified) (a)–(c); schematic view of the operation of the TENG (d) and (e and f) V_{OC} and I_{SC} curves of the resulting devices. Reprinted with permission from ref. 52. Copyright 2019 American Chemical Society.

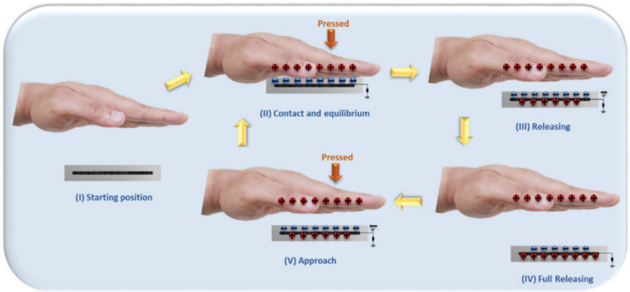

Fig. 5 Schematic representation of a complete cycle of charge generation/separation in a TENG of polypyrrole-modified textile. Reprinted with permission from ref. 85. Copyright 2022 American Chemical Society.

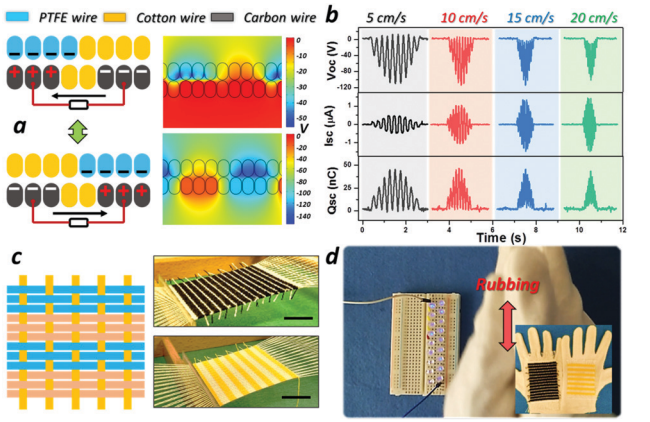

Fig. 6 (a) Scheme of the free-standing mode PTFE grating textile and interdigital carbon textile electrode for horizontal motion, (b) measurements of Voc, Isc, and Qsc under operation, (c and d) photographs of the electrode and sliding textile under operation with commercial blue LEDs. Reprinted from ref. 86. Copyright (2018), with permission from Elsevier.

advantage for the implementation of metal-free TENGs, that explore the skin as an active layer and a primary electrode for the device.

As an alternative to the conventional assembly explored for S-TENG in Fig. 4, it is possible to substitute a polymeric tribolayer by the skin that acts as an electron transfer layer. In the paper recently published by our group (see Fig. 5 for a schematic view of the device), an S-TENG is assembled with a modified textile prepared from the deposition of polypyrrole on textile in contact with a layer of Ecoflex.[85]

Independent triboelectric layer mode (I mode)

The independent TENG mode is typically explored from two different configurations: a moving triboelectric layer that slides between fixed electrodes (introducing the possibility for the development of non-contact sliding generation) and face-to-face pairs that can move up-and-down introducing variation in the vertical contact–separation mode. An important configuration to be considered is the rotating-disk mode for TENG in which the circular movement of disks provokes periodic sliding/contact modes of TENG operation, facilitating the conversion of rotatory mechanical energy into electric energy.

As an example of this mode, a free-standing TENG based on dielectric textile by PTFE and cotton threads is schematically drawn in Fig. 6(a). Results for the one-way sliding cycle operation of the device are shown in Fig. 6(b) while photos for the grating structure are shown in Fig. 6(c) and (d) (reprinted with permission from ref. 86).

As observed in the literature, there are several advantages of applying VS and SE modes in metal-free assemblies while modes I and S favor the metal-based assemblies. Based on this matching of conditions, there are many applications for metal-free TENGs based on these configurations, described in the following section.

The influence of the mode of operation and the nature of electrodes on the performance of TENGs

The development of wearable and multifunctional devices (also able to harvest energy) requires the use of stretchable and flexible supports, as represented by elastomeric supports. For metal-based structures, the physical vapor deposition introduces a metal coating layer on flexible supports to be explored as an electrode layer,[54] but at the cost of the disadvantages described in the Introduction.[87] To circumvent these drawbacks, several strategies have been drawn to substitute metal in electrodes by conducting polymers, carbon derivatives, hydrogels, and ionogels introducing relevant aspects concerning the chemical and thermal stability, low cost of production, the high electric conductivity of free-of-binders templates, and with superior mechanical strength.[54] The chemical modification of stretchable and wearable templates is observed from the coating layer deposition of additives on elastomers or textiles, the production of electrospun nets with required properties for TENGs, and more elaborated processes such as the production of coaxial TENGs.

In general, the most common assemblies for wearable and metal-free TENGs are the direct coating of conducting fillers on elastomeric supports, the modification of elastomers, and the production of electrospun nets of fibers, and the development of coaxial TENGs, which are described as follows.

Coating by conducting polymers

The modification of electrodes by incorporation of conducting polymers in elastomers represents a conventional method for the adaptation of flexibility of support and the conductivity of the filler. Wen *et al.*[88] explored the poly(dimethylsiloxane) – PDMS as an elastomeric support to grow wrinkled films of poly(3-4-ethylene dioxythiophene) – PEDOT and poly(4-styrene sulfonate) – PSS as a transparent and conductive layer for the electrode.

In correspondence to the incorporation of PEDOT-PSS in elastomers, the chemical modification of textiles with polypyrrole and polyaniline introduces advantages for the resulting all-polymer TENG in terms of high-flexibility, biocompatibility, and good mechanical properties in cost-effective structures with eco-friendly behavior. In addition to these intrinsic properties of conducting polymers, applications of TENGs tend to be extremely dependent on the self-healing properties of

materials, affecting the durability of the device (in consequence of a sequence of mechanical efforts). It is worth mentioning that different strategies must be conducted to reach desirable conditions of breathability and waterproof properties for a conducting polymer since these characteristics have been considered key to the comfortability of wearable devices such as from the coating of conducting polymers on composite aerogels.[89]

Self-healable structures of polyaniline–polypyrrole nanoflakes were explored to avoid the effects of mechanical failures after steps of successive deformation under operation.[11] Conventional supports with self-healable behaviors are introduced with organohydrogels crosslinked with phytic acid and coated with PEDOT:PSS as an active conductive layer.[90] An alternative to the substitution of conducting polymers is explored through the use of ionic hydrogels applied mutually as an electrification layer and electrode.[91] For applications in which transparency and stretchable-freezing tolerant devices are required, conductive gelatin/NaCl organohydrogels[92] introduce long-term stability in association with freezing resistance and self-healing properties. Alternatively, ionic-liquid-locked ionogel-based samples have been mutually explored as electrode and electrification layers.[93]

Electrospun-based assemblies and coaxial fibers

An alternative to electrospun-based TENGs was investigated from experimental systems in which electrospun fibers of silk fibroin and poly(vinylidene fluoride) – PVDF are deposited on conductive fibers, associated with piezoelectric and triboelectric effects.[6]

Coaxial triboelectric nanogenerators were produced on a PDMS fiber substrate and two-multi layer aligned carbon nanotubes were applied as inner and outer electrodes exploring poly(methyl methacrylate) – PMMA as a tribopair.[94] The direct modification of cotton textiles with PDMS for the following chemical polymerization of PPy represents an important step in the production of highly flexible and conducting electrodes for TENGs.

As can be seen, the performance and the wearability of TENGs depend on different parameters that vary from constitutive materials, operation mode, choice of triboelectric pairs, and the conductivity of electrodes.

This complex and delicate balance of preparation conditions for the metal-free TENGs concentrates applications into two specific operation modes (single electrode and vertical contact–separation mode) exploring the modification in the flexible electrodes by impregnation with conductive fillers (conducting polymer and carbon derivatives: carbon nanotubes, activated carbon and graphene). A diversity of applications has been observed for metal-free TENGs, such as their use in electronic devices,[65,66] self-powered sensors,[52,57] sensitive e-skin sensors and sensitive epidermal controllers,[95] robotic control and CO_2 sensing,[14] touch sensors,[56] self-powered touch/gesture sensors,[96] and so on.

Table 1 summarizes the dependence of the mode of operation, type of conductive filler for electrodes and the resulting power output, current of short circuit, and voltage of open circuit for metal-free TENGs reported in the literature.

For comparison with standard TENG devices, the response of conventional wearable TENGs making use of metal electrodes is shown in Table 2.

As can be seen, a diversity of operation modes is observed for metal-based electrodes for TENGs with the prevailing implementation of VS mode devices. Using this aspect, the

Table 1 Performance of different wearable TENGs operating with metal-free electrodes (CF = conductive fabric)

Mode	Electrode	V_{OC} (V)	I_{SC} (μA)	P (mW cm^{-2})	Ref.
Vert. cont. separ. (VS)	CF	1403	780	1.06	97
	PANI	1000	200	1.72	57
	PEDOT:PSS	540	0.787	2×10^{-1}	14
	CF	500	12	3.10×10^{-1}	6
	PPy NW	351	3.4×10^{-2}	—	55
	PANI	350	4.5×10^{-2}	1.13	56
	PPy	200	6	8.2×10^{-2}	52
	CNT	145	6.4	—	98
	MO-PPy@CLF	129	7.0	—	99
	Carbon wire	175	8.0	—	86
	Carbon film	115.2	20	1.52×10^{-1}	65
	Graphene	100	5	—	100
	BC-CNT-PPy	29	0.6	0.83×10^{-4}	101
Single Electrode	PPy	670	17.2	4.61×10^{-1}	85
	C-coffee ground	150	2.1	6.38×10^{-3}	95
	Waterproof fabric	135	7.5	6.32×10^{-2}	102
	Graphene oxide (GO)	123.1	18.61	4.97×10^{-1}	66
	PPy	60	8.8	8.3×10^{-2}	5
	Graphene	47.1	7	1.44×10^{-2}	103
	Carbon fiber	42.9	0.51	0.6×10^{-3}	104
	Organogel	40	1.2	4.0×10^{-3}	105
	Graphene	30.8	1.1	2.25×10^{-2}	67
	CNT	7	0.18	—	96
Freestanding mode	Carbon wire	118	1.5	—	86

Table 2 Performance of different wearable TENGs operating with metal-based electrodes

Mode	Electrode	V_{OC} (V)	I_{SC} (μA)	P (mW cm^{-2})	Ref.
VS	Cu	71	0.7	(56 μW)	106
	Cu	500	4	0.10	107
	Ag-nylon yarn	174	7.5	2.75×10^{-2}	108
	Ni	8.3	—	—	109
	Au	124.6	10.13	0.22	47
	Cu	12.6	0.15	—	36
	Ni	40	5	2.42	110
	Al	196	4.5	1.1×10^{-2}	9
	Pani@WCT	350	45	1.13	111
	Stainless steel fibers	200	200	1.4×10^{-3}	35
	Ag	80	4	1.1×10^{-3}	112
	Al	200	1.1	3.1×10^{-3}	113
	Al	480	75	4.6×10^{-3}	8
	Ni	50	4	3.93×10^{-2}	38
	Al	760	51	0.77	114
	Al	130	14	0.28	115
	Cu	9	0.122	—	116
	Al	124	18.7	6.09×10^{-2}	117
	MME/Al	175.77	4.65	8.5×10^{-2}	118
	Ag NW/Al	162	42	0.125	119
	Al	260	27	—	120
	Al	150	1.02	1.57×10^{-3}	121
	Cu NWs/RGO	125	2.3	7.3×10^{-2}	122
I	Cu	200	750	—	123
	Al	0.6	—	—	124
	Ag	62.9 (RMS)	1.77	5×10^{-4}	125
	Al	600	20	—	126
	Stainless steel	166	8.5	9.3×10^{-3}	127
SM	Cu/Al	190	2040	—	128
	Cu	270	11	2.5	129
	Ga/Cu	206	28.7	3.04×10^{-3}	130
	Ag-MXene	38	1.5	7×10^{-4}	131
	LM-Ag flakes-SEBS	85	4	2.19×10^{-2}	132
	Coil spring	21	0.1	—	133
SE	Stainless–steel	75	1.2	6.0×10^{-3}	13
	Ni	49	1.8	9×10^{-3}	37
	Stainless steel	150	2.9	8.5×10^{-3}	4
	Cu	870	60	0.8	134
	Cu	465.63	26.04	0.208	135
	Cu	120	9.5	0.12	136

data from the tables for power output, current of short circuit, and voltage of open circuit for metal-based and metal-free devices (VS mode) were plotted for comparison of performance. Fig. 7(a)–(c) summarize the V_{OC}, I_{SC}, and output power data for two groups of samples. As can be seen, there is no difference in the overall response of devices, with groups in black for metal-based samples and in red for samples prepared with metal-free electrodes. As shown, the variation of V_{OC} is in the range of 10 to 1000 V, with I_{SC} in the range of 10^{-7} A to 10^{-3} A and power output in the range of 10^{-3} to 10^{0} mW cm^{-2} and is the same for all of the groups.

These results confirm that the corresponding level of the electrical output range in terms of power, voltage, and current is observed for metal-free and conventional TENGs; revealing that the low conductivity level for metal-free electrodes is conveniently circumvented by filler that introduces several mechanical advantages for the skin contact. In terms of the costs, several factors must be considered for the scale-up

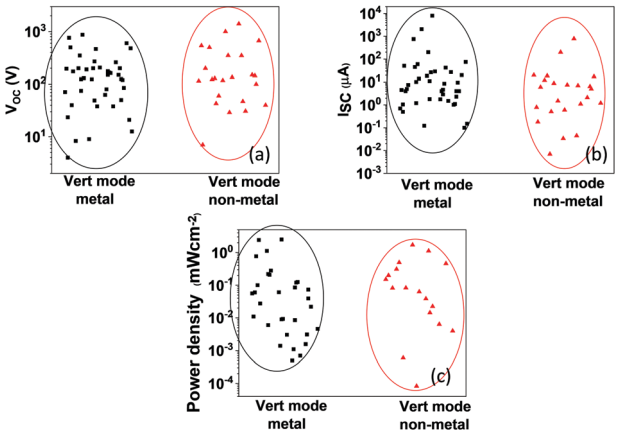

Fig. 7 Comparison of the responses summarized in Tables 1 and 2 for the vertical mode of operation for metal-based devices (in black) and no-metal-based devices (in red) for V_{OC} (a), I_{SC} (b), and power output (c).

production of TENGs. The output power, size, meantime to failure, efficiency, and type of materials are some of the critical parameters to be evaluated in the fabrication process. The substitution of metal films with metal-free (or green) materials has been considered an environmentally friendly procedure since the use of cellulose-based materials introduces advantages relative to the mass production capacity with a direct impact on the production costs.[137]

All-in-one devices and perspectives for wearable TENGs-based applications

The conversion of low frequency from irregular mechanical movement by a TENG into the pulsed power output and the following use in devices depends on the integration of energy harvesting components with energy storage devices. As a consequence, the connection of the electric signal output from a TENG to a rectification device and a storage unity (conventional capacitor/battery/supercapacitor) is critical.[57,95,111]

The assembly of the harvesting-storage-in-one system is based on the integration of TENGs and energy storage devices according to several different strategies. One of the most simple procedures is observed from the association of a TENG and supercapacitor,[5] in which an environmentally friendly procedure explored cellulose paper coated with polypyrrole mutually as a positive friction layer and an electrode connected to a bridge rectifier and symmetric supercapacitor with the same electrode of PPy/cellulose applied in the TENG. As an alternative to the use of cellulose, the deposition of polypyrrole on cotton textile coated by a PDMS layer results in an efficient device connected to a rectifier and a conventional capacitor and disposed to drive small electronics such as a digital watch.[87]

In all of the situations, the big challenge to be considered in TENG-supercapacitor-in-one self-powered sources is the use of a unique manufacturing technology. The use of 3D printing technology using resin and an ionic hydrogel as a template for mutual use in electrification layers and electrodes are completely described in ref. 138. More elaborated assemblies

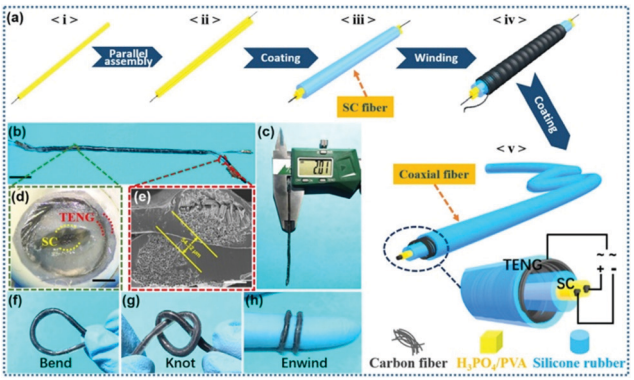

Fig. 8 Schematic diagram of a coaxial assembly of TENG-supercapacitor-in-one device (a) and mechanical properties of the coaxial TENG and SC fiber (b–h). Reprinted with permission from ref. 104. Copyright 2018 American Chemical Society.

of integrated devices are obtained from the production of coaxial fibers in which energy harvesting and storage can be explored in an integrated fiber,[104] as schematically drawn in Fig. 8.

The advantage of this system regards the compact distribution in a coaxial assembly of TENG and supercapacitor, introducing the possibility of association of fibers to improve the power output of the resulting system.

In terms of the future perspective for TENGs, the development of more efficient TENGs opens new possibilities for the technology of wearables and implantable. The boost in the performance of these devices as energy harvesting components can be considered in two specific conditions: TENGs associated with energy storage devices and active free-of-batteries sensors. For both sets of applications, there are advantages and bottlenecks to be considered to boost the performance of the resulting devices, described as follows.

For wearable-based technologies, the boost in the performance of TENGs can be explored to power up mobile phones, tablets, and electronics,[139] resulting in advances in wireless communications with the possibility to drive commercial Bluetooth devices,[140] and reinforcing the development of bionics (prototypes in soft robotics and electronics skin)[140] and self-powered smart systems.[141] The big challenge for the integration of TENG-supercapacitor-in-one devices that needs to be focused on is the improvement of isolated components and also in the integration strategies. For this, investigations focused on the boost of the output power, energy density, and stability of the TENGs is required. In terms of the optimization in the response of the coupled components, the efficiency of energy transference between parts needs to be optimized, avoiding events of impedance mismatching of devices.[82]

Another important advance in all-in-one devices is the elimination of a rectifier bridge between TENGs and energy storage devices. For this, the investigation of Li-ion batteries to evaluate ion diffusion and transport under pulsed input is necessary.[82] Relative to the use of TENGs as active sensing elements, the development of independent unities (without energy storage unities) introduces important implications in human–machine interactive systems[139] with a relevant contribution for implantable triboelectric active sensors applied (as an example) in respiratory monitoring.[140] In addition, the biomedical field can be favored by characteristic pulsed power output that can be addressed for applications in wound healing and muscle stimulation.[76]

Conclusions

The development of triboelectric nanogenerators integrated with energy storage devices and as independent active sensing devices represents a very promising strategy applied in the conversion of mechanical movements into pulsed electric energy. The adequate coupling of TENGs and energy storage devices makes possible the DC power up of conventional electronic devices from truly flexible and integrated harvesting systems with the body. The substitution of metal in electrodes by carbon derivatives and conducting polymers improves the wearability of devices while making possible the use of a common substrate as an active tribolayer and contact for TENGs and supercapacitors. More elaborated strategies applied in the production of coaxial TENG/supercapacitor in textile fibers make possible the interaction of core/shell structures for the following step of association of fibers to reach desirable energy and power output. On the other hand, the use of TENGs as active components for motion detectors opens possibilities for the production of implantable ones, with a self-powered structure that inhibits interventions for removal/change of depleted energy storage devices. The self-healable behavior and the integration with textiles are important advantages for metal-free electrodes that must combine these characteristics with breathability and waterproof properties in highly conductive structures (truly incorporated in textiles) with the ability to preserve properties under extreme mechanical efforts and washing procedures.

Author contributions

CRediT: G. S. Oliveira: Conceptualization, investigation, methodology, writing – original draft; I. C. M. Candido: Conceptualization, investigation, methodology H. P. de Oliveira: Conceptualization, funding acquisition, investigation, methodology, writing – review & editing.

Conflicts of interest

There are no conflicts to declare.

Acknowledgements

This work was supported by CAPES, FAPESB, FACEPE, FINEP, and CNPq.

Notes and references

1 S. A. Graham, B. Dudem, A. R. Mule, H. Patnam and J. S. Yu, *Nano Energy*, 2019, **61**, 505–516.
2 B. Dudem, D. H. Kim, A. R. Mule and J. S. Yu, *ACS Appl. Mater. Interfaces*, 2018, **10**, 24181–24192.
3 B. Dudem, Y. H. Ko, J. W. Leem, S. H. Lee and J. S. Yu, *ACS Appl. Mater. Interfaces*, 2015, **7**, 20520–20529.
4 K. Dong, Y. C. Wang, J. Deng, Y. Dai, S. L. Zhang, H. Zou, B. Gu, B. Sun and Z. L. Wang, *ACS Nano*, 2017, **11**, 9490–9499.
5 X. Shi, S. Chen, H. Zhang, J. Jiang, Z. Ma and S. Gong, *ACS Sustainable Chem. Eng.*, 2019, **7**, 18657–18666.
6 Y. Guo, X. S. Zhang, Y. Wang, W. Gong, Q. Zhang, H. Wang and J. Brugger, *Nano Energy*, 2018, **48**, 152–160.
7 J. Liu, L. Gu, N. Cui, Q. Xu, Y. Qin and R. Yang, *Research*, 2019, **2019**, 1–13.
8 X. Cheng, Y. Song, M. Han, B. Meng, Z. Su, L. Miao and H. Zhang, *Sens. Actuators, A.*, 2016, **247**, 206–214.
9 M. Zhu, Q. Shi, T. He, Z. Yi, Y. Ma, B. Yang, T. Chen and C. Lee, *ACS Nano*, 2019, **13**, 1940–1952.
10 T. Zhao, J. Li, H. Zeng, Y. Fu, H. He, L. Xing, Y. Zhang and X. Xue, *Nanotechnology*, 2018, **29**, 405504.
11 S. Singh, R. K. Tripathi, M. K. Gupta, G. I. Dzhardimalieva, I. E. Uflyand and B. C. Yadav, *J. Colloid Interface Sci.*, 2021, **600**, 572–585.
12 S. S. Kwak, H. Kim, W. Seung, J. Kim, R. Hinchet and S. W. Kim, *ACS Nano*, 2017, **11**, 10733–10741.
13 A. Yu, X. Pu, R. Wen, M. Liu, T. Zhou, K. Zhang, Y. Zhang, J. Zhai, W. Hu and Z. L. Wang, *ACS Nano*, 2017, **11**, 12764–12771.
14 T. He, Q. Shi, H. Wang, F. Wen, T. Chen, J. Ouyang and C. Lee, *Nano Energy*, 2019, **57**, 338–352.
15 F.-R. Fan, Z.-Q. Tian and Z. Lin Wang, *Nano Energy*, 2012, **1**, 328–334.
16 Z. Bai, Y. Xu, J. Li, J. Zhu, C. Gao, Y. Zhang, J. Wang and J. Guo, *ACS Appl. Mater. Interfaces*, 2020, **12**, 42880–42890.
17 Y. Liu, Y. Zheng, Z. Wu, L. Zhang, W. Sun, T. Li, D. Wang and F. Zhou, *Nano Energy*, 2020, 105422.
18 H. Wang, M. Shi, K. Zhu, Z. Su, X. Cheng, Y. Song, X. Chen, Z. Liao, M. Zhang and H. Zhang, *Nanoscale*, 2016, **8**, 18489–18494.
19 Z. Zhang and J. Cai, *Curr. Appl. Phys.*, 2021, **22**, 1–5.
20 S. Paria, S. K. Si, S. K. Karan, A. K. Das, A. Maitra, R. Bera, L. Halder, A. Bera, A. De and B. B. Khatua, *J. Mater. Chem. A*, 2019, **7**, 3979–3991.
21 Q. Jing, Y. Xie, G. Zhu, R. P. S. Han and Z. L. Wang, *Nat. Commun.*, 2015, **6**, 1–8.
22 S. Wang, L. Lin and Z. L. Wang, *Nano Energy*, 2015, **11**, 436–462.
23 C. García Núñez, L. Manjakkal and R. Dahiya, *npj Flexible Electron.*, 2019, **3**, 1.
24 W. Jiang, H. Li, Z. Liu, Z. Li, J. Tian, B. Shi, Y. Zou, H. Ouyang, C. Zhao, L. Zhao, R. Sun, H. Zheng, Y. Fan, Z. L. Wang and Z. Li, *Adv. Mater.*, 2018, **30**, 1801895.
25 Z. Li, H. Feng, Q. Zheng, H. Li, C. Zhao, H. Ouyang, S. Noreen, M. Yu, F. Su, R. Liu, L. Li, Z. L. Wang and Z. Li, *Nano Energy*, 2018, **54**, 390–399.
26 R. Wang, S. Gao, Z. Yang, Y. Li, W. Chen, B. Wu and W. Wu, *Adv. Mater.*, 2018, **30**, 1706267.
27 Y. Zou, L. Bo and Z. Li, *Fundam. Res.*, 2021, **1**, 364–382.
28 X. Qu, X. Ma, B. Shi, H. Li, L. Zheng, C. Wang, Z. Liu, Y. Fan, X. Chen, Z. Li and Z. L. Wang, *Adv. Funct. Mater.*, 2021, **31**, 2006612.
29 G. Zhu, Z. H. Lin, Q. Jing, P. Bai, C. Pan, Y. Yang, Y. Zhou and Z. L. Wang, *Nano Lett.*, 2013, **13**, 847–853.
30 G. Zhu, C. Pan, W. Guo, C. Y. Chen, Y. Zhou, R. Yu and Z. L. Wang, *Nano Lett.*, 2012, **12**, 4960–4965.
31 Zeeshan, R. Ahmed, W. Chun, S. J. Oh and Y. Kim, *Energies*, 2019, **12**, 1774.
32 T. Li, Y. Xu, M. Willander, F. Xing, X. Cao, N. Wang and Z. L. Wang, *Adv. Funct. Mater.*, 2016, **26**, 4370–4376.
33 S. Yan, Z. Zhang, X. Shi, Y. Xu, Y. Li, X. Wang, Q. Li and L. S. Turng, *Int. J. Energy Res.*, 2021, **45**, 11053–11064.
34 C. Chen, H. Guo, L. Chen, Y. C. Wang, X. Pu, W. Yu, F. Wang, Z. Du and Z. L. Wang, *ACS Nano*, 2020, **14**, 4585–4594.
35 Y. C. Lai, J. Deng, S. L. Zhang, S. Niu, H. Guo and Z. L. Wang, *Adv. Funct. Mater.*, 2017, **27**, 1604462.
36 Z. Wen, M. H. Yeh, H. Guo, J. Wang, Y. Zi, W. Xu, J. Deng, L. Zhu, X. Wang, C. Hu, L. Zhu, X. Sun and Z. L. Wang, *Sci. Adv.*, 2016, **2**, 1600097.
37 Z. Cong, Z. Cong, W. Guo, W. Guo, Z. Guo, Z. Guo, Y. Chen, Y. Chen, M. Liu, M. Liu, T. Hou, T. Hou, X. Pu, X. Pu, X. Pu, W. Hu, W. Hu, W. Hu, Z. L. Wang, Z. L. Wang, Z. L. Wang and Z. L. Wang, *ACS Nano*, 2020, **14**, 5590–5599.
38 X. Pu, L. Li, H. Song, C. Du, Z. Zhao, C. Jiang, G. Cao, W. Hu and Z. L. Wang, *Adv. Mater.*, 2015, **27**, 2472–2478.
39 Y. Xi, J. Hua and Y. Shi, *Nano Energy*, 2020, **69**, 104390.
40 T. Cheng, Q. Gao and Z. L. Wang, *Adv. Mater. Technol.*, 2019, **4**, 1800588.
41 J. Huang, X. Fu, G. Liu, S. Xu, X. Li, C. Zhang and L. Jiang, *Nano Energy*, 2019, **62**, 638–644.
42 L. Zhang, L. Jin, B. Zhang, W. Deng, H. Pan, J. Tang, M. Zhu and W. Yang, *Nano Energy*, 2015, **16**, 516–523.
43 S. Wang, Y. Xie, S. Niu, L. Lin and Z. L. Wang, *Adv. Mater.*, 2014, **26**, 2818–2824.
44 W. Zhong, L. Xu, X. Yang, W. Tang, J. Shao, B. Chen and Z. L. Wang, *Nanoscale*, 2019, **11**, 7199–7208.
45 M. Su, J. Brugger and B. Kim, *Int. J. Precis. Eng. Manuf. – Green Technol.*, 2020, **7**, 683–698.
46 D. Kim, S. B. Jeon, J. Y. Kim, M. L. Seol, S. O. Kim and Y. K. Choi, *Nano Energy*, 2015, **12**, 331–338.
47 H. Chen, L. Bai, T. Li, C. Zhao, J. Zhang, N. Zhang, G. Song, Q. Gan and Y. Xu, *Nano Energy*, 2018, **46**, 73–80.
48 S. J. Park, M. L. Seol, S. B. Jeon, D. Kim, D. Lee and Y. K. Choi, *Sci. Rep.*, 2015, **5**, 13866.
49 J. H. Lee, R. Hinchet, S. K. Kim, S. Kim and S. W. Kim, *Energy Environ. Sci.*, 2015, **8**, 3605–3613.
50 A. Taghizadeh, M. Taghizadeh, M. Jouyandeh, M. K. Yazdi, P. Zarrintaj, M. R. Saeb, E. C. Lima and V. K. Gupta, *J. Mol. Liq.*, 2020, **312**, 113447.
51 G. Prunet, F. Pawula, G. Fleury, E. Cloutet, A. J. Robinson, G. Hadziioannou and A. Pakdel, *Mater. Today Phys.*, 2021, **18**, 100402.

52 A. R. Mule, B. Dudem, H. Patnam, S. A. Graham and J. S. Yu, *ACS Sustainable Chem. Eng.*, 2019, **7**, 16450–16458.
53 C. Wang, X. Qu, Q. Zheng, Y. Liu, P. Tan, B. Shi, H. Ouyang, S. Chao, Y. Zou, C. Zhao, Z. Liu, Y. Li and Z. Li, *ACS Nano*, 2021, **15**, 10130–10140.
54 J. Wang, Z. Wen, Y. Zi, P. Zhou, J. Lin, H. Guo, Y. Xu and Z. L. Wang, *Adv. Funct. Mater.*, 2016, **26**, 1070–1076.
55 S. Cui, Y. Zheng, J. Liang and D. Wang, *Chem. Sci.*, 2016, **7**, 6477–6483.
56 B. Dudem, A. R. Mule, H. R. Patnam and J. S. Yu, *Nano Energy*, 2019, **55**, 305–315.
57 H. J. Qiu, W. Z. Song, X. X. Wang, J. Zhang, Z. Fan, M. Yu, S. Ramakrishna and Y. Z. Long, *Nano Energy*, 2019, **58**, 536–542.
58 Z. Li, G. Ma, R. Ge, F. Qin, X. Dong, W. Meng, T. Liu, J. Tong, F. Jiang, Y. Zhou, K. Li, X. Min, K. Huo and Y. Zhou, *Angew. Chem., Int. Ed.*, 2016, **128**, 991–994.
59 B. Y. Lee, S. U. Kim, S. Kang and S. D. Lee, *Nano Energy*, 2018, **53**, 152–159.
60 J. Shi, X. Chen, G. Li, N. Sun, H. Jiang, D. Bao, L. Xie, M. Peng, Y. Liu, Z. Wen and X. Sun, *Nanoscale*, 2019, **11**, 7513–7519.
61 H. P. De Oliveira and C. P. De Melo, *Synth. Methods*, 2006, **156**, 215–218.
62 L. Zhang, M. Fairbanks and T. L. Andrew, *Adv. Funct. Mater.*, 2017, **27**, 1700415.
63 G. Qi, L. Huang and H. Wang, *Chem. Commun.*, 2012, **48**, 8246–8248.
64 R. M. A. P. Lima, J. J. Alcaraz-Espinoza, F. A. G. Da Silva and H. P. De Oliveira, *ACS Appl. Mater. Interfaces*, 2018, **10**, 13783–13795.
65 J. Liu, D. Yu, Z. Zheng, G. Huangfu and Y. Guo, *Ceram. Int.*, 2021, **47**, 3573–3579.
66 Y. Wu, Y. Luo, J. Qu, W. A. Daoud and T. Qi, *Nano Energy*, 2019, **64**, 103948.
67 E. He, Y. Sun, X. Wang, H. Chen, B. Sun, B. Gu and W. Zhang, *Composites, Part B*, 2020, **200**, 108244.
68 J. Wang, Z. Wen, Y. Zi, P. Zhou, J. Lin, H. Guo, Y. Xu and Z. L. Wang, *Adv. Funct. Mater.*, 2016, **26**, 1070–1076.
69 R. M. A. P. Lima, M. C. A. de Oliveira and H. P. de Oliveira, *SN Appl. Sci.*, 2019, **1**, 325.
70 R. Moreno Araújo Pinheiro Lima and H. P. de Oliveira, *J. Energy Storage*, 2020, **28**, 101284.
71 G. S. dos Reis, R. M. A. Pinheiro Lima, S. H. Larsson, C. M. Subramaniyam, V. M. Dinh, M. Thyrel and H. P. de Oliveira, *J. Environ. Chem. Eng.*, 2021, **9**, 106155.
72 J. J. Alcaraz-Espinoza, C. P. De Melo and H. P. De Oliveira, *ACS Omega*, 2017, **2**, 2866–2877.
73 N. Siraj, S. Macchi, B. Berry and T. Viswanathan, *Electrochem*, 2020, **1**, 410–438.
74 Y. Xu, Y. Tao, X. Zheng, H. Ma, J. Luo, F. Kang and Q. H. Yang, *Adv. Mater.*, 2015, **27**, 8082–8087.
75 H. Hwang, K. Y. Lee, D. Shin, J. Shin, S. Kim and W. Choi, *Appl. Surf. Sci.*, 2018, **442**, 693–699.
76 Y. Zhou, W. Deng, J. Xu and J. Chen, *Cell Rep. Phys. Sci.*, 2020, **1**, 100142.
77 C. Wu, A. C. Wang, W. Ding, H. Guo and Z. L. Wang, *Adv. Energy Mater.*, 2019, **9**, 1–25.
78 H. Patnam, B. Dudem, S. A. Graham and J. S. Yu, *Energy*, 2021, **223**, 120031.
79 F. G. Torres and G. E. De-la-Torre, *Carbohydr. Polym.*, 2021, **251**, 117055.
80 H. P. de Oliveira, *Electrochem*, 2021, **2**, 118–134.
81 Z. L. Wang, *Faraday Discuss.*, 2014, **176**, 447–458.
82 J. Luo and Z. L. Wang, *Energy Storage Mater.*, 2019, **23**, 617–628.
83 R. D. I. G. Dharmasena, *Nano Energy*, 2020, **76**, 105045.
84 M. R. dos Santos, J. J. Alcaraz-Espinoza, M. M. da Costa and H. P. de Oliveira, *Mater. Sci. Eng., C*, 2018, **89**, 33–40.
85 I. C. M. Candido, G. D. S. Oliveira, G. G. Viana, F. A. G. Da Silva, M. M. Da Costa and H. P. De Oliveira, *ACS Appl. Electron. Mater.*, 2022, **4**, 334–344.
86 J. Chen, H. Guo, X. Pu, X. Wang, Y. Xi and C. Hu, *Nano Energy*, 2018, **50**, 536–543.
87 A. R. Mule, B. Dudem, H. Patnam, S. A. Graham and J. S. Yu, *ACS Sustainable Chem. Eng.*, 2019, **7**, 16450–16458.
88 Z. Wen, Y. Yang, N. Sun, G. Li, Y. Liu, C. Chen, J. Shi, L. Xie, H. Jiang, D. Bao, Q. Zhuo and X. Sun, *Adv. Funct. Mater.*, 2018, **28**, 1803684.
89 Y. Wang, L. Chen, H. Cheng, B. Wang, X. Feng, Z. Mao and X. Sui, *Chem. – Eng. J.*, 2020, **402**, 126222.
90 A. Khan, S. Ginnaram, C. H. Wu, H. W. Lu, Y. F. Pu, J. I. Wu, D. Gupta, Y. C. Lai and H. C. Lin, *Nano Energy*, 2021, **90**, 106525.
91 X. Pu, M. Liu, X. Chen, J. Sun, C. Du, Y. Zhang, J. Zhai, W. Hu and Z. L. Wang, *Sci. Adv.*, 2017, **3**, e1700015.
92 M. Wu, X. Wang, Y. Xia, Y. Zhu, S. Zhu, C. Jia, W. Guo, Q. Li and Z. Yan, *Nano Energy*, 2022, **95**, 106967.
93 G. Zhao, Y. Zhang, N. Shi, Z. Liu, X. Zhang, M. Wu, C. Pan, H. Liu, L. Li and Z. L. Wang, *Nano Energy*, 2019, **59**, 302–310.
94 X. Yu, J. Pan, J. Zhang, H. Sun, S. He, L. Qiu, H. Lou, X. Sun and H. Peng, *J. Mater. Chem. A*, 2017, **5**, 6032–6037.
95 M. Li, W. Y. Cheng, Y. C. Li, H. M. Wu, Y. C. Wu, H. W. Lu, S. L. Cheng, L. Li, K. C. Chang, H. J. Liu, Y. F. Lin, L. Y. Lin and Y. C. Lai, *Nano Energy*, 2021, **79**, 105405.
96 R. Cao, X. Pu, X. Du, W. Yang, J. Wang, H. Guo, S. Zhao, Z. Yuan, C. Zhang, C. Li and Z. L. Wang, *ACS Nano*, 2018, **12**, 5190–5196.
97 J. H. Zhang, Y. Li, J. Du, X. Hao and Q. Wang, *Nano Energy*, 2019, **61**, 486–495.
98 J. Wang, S. Li, F. Yi, Y. Zi, J. Lin, X. Wang, Y. Xu and Z. L. Wang, *Nat. Commun.*, 2016, **7**, 12744.
99 Q. Li, X. An and X. Qian, *Polymers*, 2022, **14**, 332.
100 I. J. Chung, W. Kim, W. Jang, H. W. Park, A. Sohn, K. B. Chung, D. W. Kim, D. Choi and Y. T. Park, *J. Mater. Chem. A*, 2018, **6**, 3108–3115.
101 J. Zhang, S. Hu, Z. Shi, Y. Wang, Y. Lei, J. Han, Y. Xiong, J. Sun, L. Zheng, Q. Sun, G. Yang and Z. L. Wang, *Nano Energy*, 2021, **89**, 106354.
102 J. Wang, J. He, L. Ma, Y. Yao, X. Zhu, L. Peng, X. Liu, K. Li and M. Qu, *Chem. – Eng. J.*, 2021, **423**, 130200.

103 H. Chu, H. Jang, Y. Lee, Y. Chae and J. H. Ahn, *Nano Energy*, 2016, **27**, 298–305.
104 Y. Yang, L. Xie, Z. Wen, C. Chen, X. Chen, A. Wei, P. Cheng, X. Xie and X. Sun, *ACS Appl. Mater. Interfaces*, 2018, **10**, 42356–42362.
105 T. Jing, B. Xu and Y. Yang, *Nano Energy*, 2021, **84**, 105867.
106 X. Tao, Y. Zhou, K. Qi, C. Guo, Y. Dai, J. He and Z. Dai, *J. Colloid Interface Sci.*, 2022, **608**, 2339–2346.
107 Q. Sun, L. Wang, X. Yue, L. Zhang, G. Ren, D. Li, H. Wang, Y. Han, L. Xiao, G. Lu, H. D. Yu and W. Huang, *Nano Energy*, 2021, **89**, 106329.
108 Y. Gao, Z. Li, B. Xu, M. Li, C. Jiang, X. Guan and Y. Yang, *Nano Energy*, 2022, **91**, 106672.
109 C. Gui, R. Zhang, Z. Chen, W. Wu, H. Li and J. Huang, *Compos. Sci. Technol.*, 2022, **218**, 109187.
110 X. Pu, L. Li, M. Liu, C. Jiang, C. Du, Z. Zhao, W. Hu and Z. L. Wang, *Adv. Mater.*, 2016, **28**, 98–105.
111 B. Dudem, A. R. Mule, H. R. Patnam and J. S. Yu, *Nano Energy*, 2019, **55**, 305–315.
112 H. Li, S. Zhao, X. Du, J. Wang, R. Cao, Y. Xing and C. Li, *Adv. Mater. Technol.*, 2018, **3**, 1800065.
113 S. Bayan, S. Pal and S. K. Ray, *Nano Energy*, 2022, **94**, 106928.
114 B.-C. Kang, H. J. Choi, S. J. Park and T. J. Ha, *Energy*, 2021, **233**, 121196.
115 Y. T. Jao, P. K. Yang, C. M. Chiu, Y. J. Lin, S. W. Chen, D. Choi and Z. H. Lin, *Nano Energy*, 2018, **50**, 513–520.
116 H. Zhang, J. Zhang, Z. Hu, L. Quan, L. Shi, J. Chen, W. Xuan, Z. Zhang, S. Dong and J. Luo, *Nano Energy*, 2019, **59**, 75–83.
117 H. Li, R. Li, X. Fang, H. Jiang, X. Ding, B. Tang, G. Zhou, R. Zhou and Y. Tang, *Nano Energy*, 2019, **58**, 447–454.
118 H. Li, Y. Sun, Y. Su, R. Li, H. Jiang, Y. Xie, X. Ding, X. Wu and Y. Tang, *Nano Energy*, 2021, **89**, 106423.
119 D. Doganay, M. O. Cicek, M. B. Durukan, B. Altuntas, E. Agbahca, S. Coskun and H. E. Unalan, *Nano Energy*, 2021, **89**, 106412.
120 D. H. Ho, J. Han, J. Huang, Y. Y. Choi, S. Cheon, J. Sun, Y. Lei, G. S. Park, Z. L. Wang, Q. Sun and J. H. Cho, *Nano Energy*, 2020, **77**, 105262.
121 J. N. Kim, J. Lee, T. W. Go, A. Rajabi-Abhari, M. Mahato, J. Y. Park, H. Lee and I. K. Oh, *Nano Energy*, 2020, **75**, 104904.
122 G. Z. Li, G. G. Wang, Y. W. Cai, N. Sun, F. Li, H. L. Zhou, H. X. Zhao, X. N. Zhang, J. C. Han and Y. Yang, *Nano Energy*, 2020, **75**, 104918.
123 S. Y. Kuang, J. Chen, X. B. Cheng, G. Zhu and Z. L. Wang, *Nano Energy*, 2015, **17**, 10–16.
124 D. Vera Anaya, T. He, C. Lee and M. R. Yuce, *Nano Energy*, 2020, **72**, 104675.
125 W. Paosangthong, M. Wagih, R. Torah and S. Beeby, *Nano Energy*, 2022, **92**, 106739.
126 Y. Yun, S. Jang, S. Cho, S. H. Lee, H. J. Hwang and D. Choi, *Nano Energy*, 2021, **80**, 105525.
127 X. Guan, B. Xu, M. Wu, T. Jing, Y. Yang and Y. Gao, *Nano Energy*, 2021, **80**, 105549.
128 M. Salauddin, R. M. Toyabur, P. Maharjan, M. S. Rasel, J. W. Kim, H. Cho and J. Y. Park, *Nano Energy*, 2018, **51**, 61–72.
129 J. Qi, A. C. Wang, W. Yang, M. Zhang, C. Hou, Q. Zhang, Y. Li and H. Wang, *Nano Energy*, 2020, **67**, 104206.
130 W. Wang, A. Yu, X. Liu, Y. Liu, Y. Zhang, Y. Zhu, Y. Lei, M. Jia, J. Zhai and Z. L. Wang, *Nano Energy*, 2020, **71**, 104605.
131 J. Liu, L. Zhang, N. Wang and C. Li, *Nano Energy*, 2020, **78**, 105385.
132 Y. Li, J. Xiong, J. Lv, J. Chen, D. Gao, X. Zhang and P. S. Lee, *Nano Energy*, 2020, **78**, 105358.
133 M. He, W. Du, Y. Feng, S. Li, W. Wang, X. Zhang, A. Yu, L. Wan and J. Zhai, *Nano Energy*, 2021, **86**, 106058.
134 M. Matsunaga, J. Hirotani, S. Kishimoto and Y. Ohno, *Nano Energy*, 2020, **67**, 104297.
135 M. Feng, Y. Wu, Y. Feng, Y. Dong, Y. Liu, J. Peng, N. Wang, S. Xu and D. Wang, *Nano Energy*, 2022, **93**, 106835.
136 Y. Hu, Y. Shi, X. Cao, Y. Liu, S. Guo and J. Shen, *Nano Energy*, 2021, **86**, 106103.
137 R. Zhang and H. Olin, *EcoMat*, 2020, **2**, e12062.
138 B. Chen, W. Tang, T. Jiang, L. Zhu, X. Chen, C. He, L. Xu, H. Guo, P. Lin, D. Li, J. Shao and Z. L. Wang, *Nano Energy*, 2018, **45**, 380–389.
139 K. Dong, X. Peng and Z. L. Wang, *Adv. Mater.*, 2020, **32**, 1–43.
140 M. Han, X. Zhang and H. Zhang, *Flexible and Stretchable Triboelectric Nanogenerator Devices: Toward Self-Powered Systems*, Wiley, 2019.
141 X. S. Zhang, M. Di Han, B. Meng and H. X. Zhang, *Nano Energy*, 2015, **11**, 304–322.